Manufacturing Letters 32 (2022) 44–48

Contents lists available at ScienceDirect

Manufacturing Letters

journal homepage: www.elsevier.com/locate/mfglet

Letters

Molten pool swing in printing the steel/inconel functionally gradient material with laser-based Directed Energy Deposition

Runyu Zhang, Ning Bian, Hongbing Lu, Yaoyu Li, Yi Tian, Wei Li *

Department of Mechanical Engineering, The University of Texas at Dallas, Richardson, TX, USA

ARTICLE INFO

Article history:
Received 1 November 2021
Received in revised form 5 February 2022
Accepted 9 March 2022
Available online 18 March 2022

Keywords:
Functionally gradient materials
Directed energy deposition
Molten pool shaking

ABSTRACT

Laser-based Directed Energy Deposition (DED) is being used increasingly for printing functionally graded materials (FGMs). In the DED process, two metal powders are blown into the molten pool. The printed functionally gradient material has layered structures with the composition ratio in each layer changing gradually. We report an interesting molten pool swing phenomenon in the DED printing of the stainless steel 316L/Inconel 718 gradient material. It is found that the molten pool moves around periodically and its light intensity changes between bright and less bright in sequence in printing the layer of 75% SS316L and 25% IN718.

1. Introduction

Functionally gradient materials (FGMs) have received increasing attention due to their unique material compositions and physical/mechanical properties. Due to their advantages in the manufacturing characteristics, especially in the ease of the control of material compositions in an FGM, laser-based Directed Energy Deposition (DED) has become an important additive manufacturing process to build metallic FGMs. To fabricate one FGM layer with a specific gradient material composition ratio, two distinct metallic powders are pre-mixed or in-situ mixed [1–6], the powder mixture is subsequently melted in the molten pool by a laser beam. The molten pool evolution and morphology in FGMs are likely different from those in the molten pool in a regular DED process in the case of printing with a uniform powder material [7]. The FGM molten pools are sensitive to the different physical properties of the powder materials, including solidus and liquidus temperatures, thermal conductivities, latent heat, viscosity, etc. [1,8]. Due to the complexity in printing FGMs with DED, to date, the reported results on FGM molten pools are sparse [7,9].

In this study, the DED process was used to fabricate stainless steel 316L/Inconel 718 FGM structure by in-situ mixing two types of powders in a coaxial nozzle. A digital camera attached to the DED machine was used to record videos of the DED process to observe the swing process from the top view. This video showing the swing process was analyzed frame by frame. After that, an optical microscope was used to observe the ripple morphology on the FGM surface caused by molten pool swing. The ripple frequency was quantified to study the molten pool swing.

2. Experiment

2.1. Experimental platform

SS316L/IN718 specimens were fabricated with an in-house laser-based (Laserline Gmbh, LDM 1000-40) DED platform based on a CNC milling machine (Tormach 1100 M) integrated with four powder feeders (PowderMotionLabs, X2W). The two types of virgin powders used in the experiment were gas atomized stainless steel 316L and Inconel 718 (PowderRange, Carpenter Additive). Images and details regarding this customized DED system and the chemical composition of these two kinds of powder are available in Supplemental Materials. The working environment was fully isolated and sealed with Argon gas to minimize oxidation. An 8-megapixel digital camera (3.95 μm/pixel) was integrated with the deposition head, to acquire videos of the molten pool evolution process during printing. The video was later post-processed so that the evolution of the molten pool during the entire printing process was revealed and analyzed. A Leica stereo optical microscope was used to observe the surface morphology of the printed FGM specimen. Multiple optical micrographs were taken at different locations of the FGM specimen to investigate the ripple morphology.

2.2. Experimental process

The processing parameters used in this DED experiment are as follows: laser power (200–800 W), powder feed rate (4 g/min),

* Corresponding author.
E-mail address: Wei.Li@UTDallas.edu (W. Li).

https://doi.org/10.1016/j.mfglet.2022.03.002

scanning speed (50 mm/min), layer thickness (1 mm), and argon gas flow (5 standard liter/min). An SS316L/IN718 FGM thin-walled specimen was fabricated with a back-and-forth printing path as shown using the red dash line in Fig. 2.

The swinging molten pool phenomenon was first observed during the DED process of fabricating the SS316L/IN718 FGM specimen shown in Fig. 1(a) with different material compositions. It was observed that the molten pool was swinging between left and right in the direction transverse to the printing path when printing the layers of "75% SS316L + 25% IN718". Fig. 1(a) shows that the ripple morphology exists in the two layers of "75% SS316L + 25% IN718", while the other layers have a relatively smooth surface finish. This also confirmed the direct observation from the in-situ camera integrated inside the nozzle that the molten pool swung left and right regularly during the process of printing these layers.

To facilitate the observation of molten pool swing, another specimen was printed with the material composition of "75% SS316L + 25% IN718" across all ten layers as shown in Fig. 1(b). The ripple morphology existed on all ten layers starting from the first one on the bottom to the top layers, which did not happen while printing a specimen with single powder composition as shown in Fig. 1(c) and (d). The videos of the molten pool while printing each of the four specimens in Fig. 1 are available in Supplemental Materials.

3. Results and discussion

3.1. Direct observations of the molten pool swing and ripple morphology on FGM surfaces

The printing process was recorded by the digital camera. Fig. 2 shows the schematic of the printing path and the molten pool swing trace in Fig. 2(a), and video frames of some of the swing movements in Fig. 2(b)–(e) for demonstrations. Fig. 2(b) – (e), consisting of a series of images with increasing timestamps as labeled, depict a complete molten pool swing process from side A to side B, and then back to side A. The instantaneous positions of the molten pool during each swing at the indicated timestamp were also represented by the dots with corresponding letters on the schematics to the left. Based on the timestamps, the equivalent molten pool swing frequency is estimated at 0.91 Hz, 1.18 Hz, 1.03 Hz, and 1.22 Hz for the second, third, fifth, and sixth layer, respectively. The swing direction was perpendicular to the printing path which was depicted with a red dash line. Those layers were picked as a representation based on the micrograph observations shown in Fig. 3 that the ripple morphology at these layers displayed distinct patterns in terms of the morphology size and the ripple frequency.

Apart from the molten pool swing, another observation from the video frames was the brightness difference during molten pool swing on the same layer as shown in Fig. 2. During each swing, the molten pool became brighter as it was shifted from one side to the middle, while became dimmer as it reached the other side.

3.2. Ripple morphology quantification by micrographs

Optical micrographs provided clear views of the surface ripple morphology of the FGM specimen as the one shown in Fig. 3(a), which were not present on specimens with single powder composition as shown in Fig. 3(b) and (c). The thickness and the ripple frequency of each layer were calculated based on the provided scale bar from the micrograph and averaged out based on values at three different spots – the left, middle, and right parts of the FGM specimen. The results are plotted in Fig. 3 for analysis. The average layer thickness and ripple frequency are distinct for all ten layers. The increasing trend of the layer thickness is considered to result from a larger molten pool that later solidifies to a thicker metal layer [8]. And the ripple frequency becomes smaller as the layer thickness grows larger. Because the ripple frequency is directly related to how quickly the molten pool swings, it is concluded that the molten pool becomes larger as it swings slower. This is especially obvious when referring to the recorded video that the molten pool swung at a much slower pace while printing layers five and six compared to a much faster pace it swung while printing the previous layers.

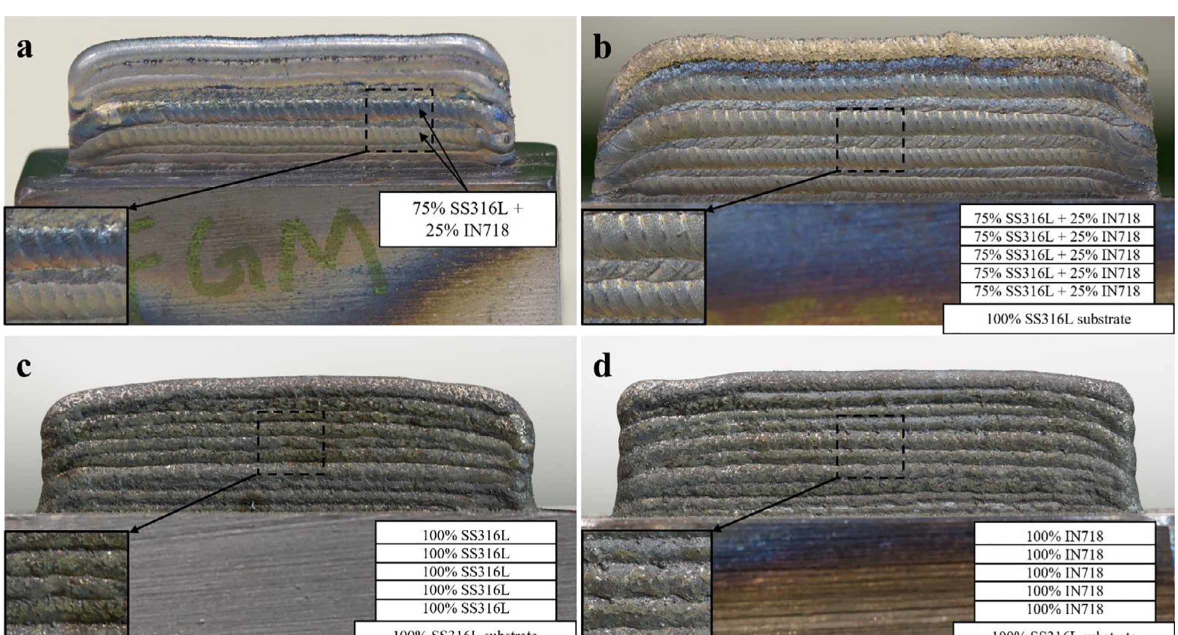

Fig. 1. Four different specimens fabricated with the DED process: a) an FGM specimen with a gradient material composition design; b) a specimen with "75% SS316L + 25% IN718" material composition design; c) a specimen with "100% SS316L" material composition; d) a specimen with "100% IN718" material composition.

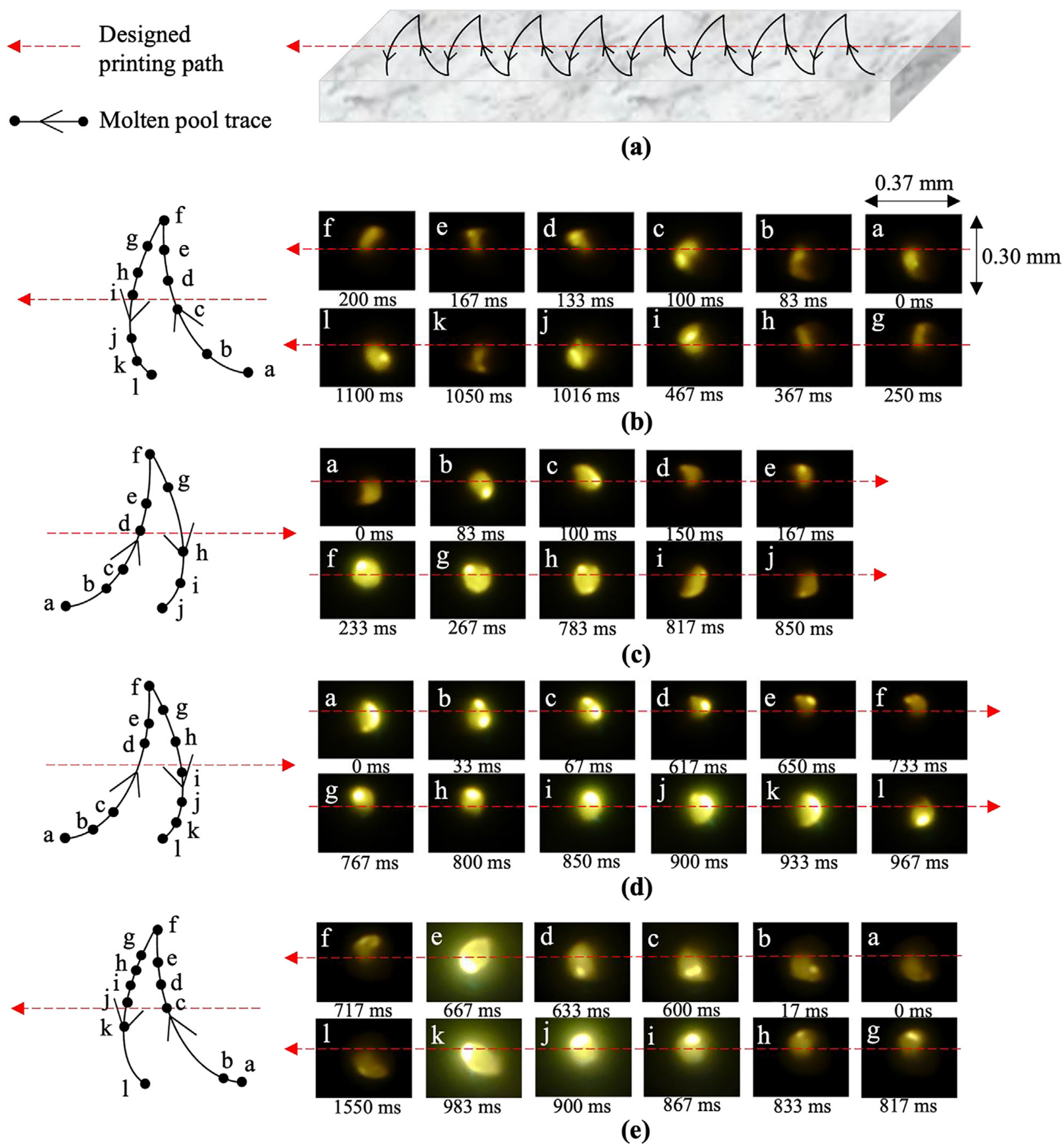

Fig. 2. Designed printing path (marked in red dash line), and molten pool trace (in solid black line). (a) A schematic showing the printing path, and the molten pool trace while printing each layer; (b)–(e) each showing one complete molten pool swing, from side A to side B, and back to side A: (b) the 2nd layer, (c) the 3rd layer, (d) the 5th layer, and (e) the 6th layer. (For interpretation of the references to colour in this figure legend, the reader is referred to the web version of this article.)

Before further investigating the causes for this molten pool swing phenomenon, efforts are made on examining the DED system and associated software used in this study. Firstly, all components in this equipment are commercially available and assembled by the manufacturer, including the precision powder feeder systems that use patented technology leveraging electrostatic forces to manipulate powder particles to provide smooth and consistent powder flow with excellent feed rate repeatability [10,11]. Secondly, the system uses the LinuxCNC software system to implement the numerical control of the entire operation. Schematics of this integrated DED system and details on its powder delivery mechanism are provided in Supplemental Materials. Also, it is found that this molten pool swing only occurs to specific material composition and range of mix ratio. Therefore, the causes for such phenomenon due to equipment and software errors have been ruled out. There exist numerous studies and theories on molten pool instability in the DED process. One important aspect is the laser energy absorption of Fe (iron) and Ni (nickel) under 1000 nm wavelength laser that is used in this study, which has an absorption coefficient of 36% and 28%, respectively [12]. Since Fe and Ni are the primary chemical composition for SS316L and IN718 powder used in this study, the laser absorption difference between them in the molten state can cause instability and changes in the brightness of the molten

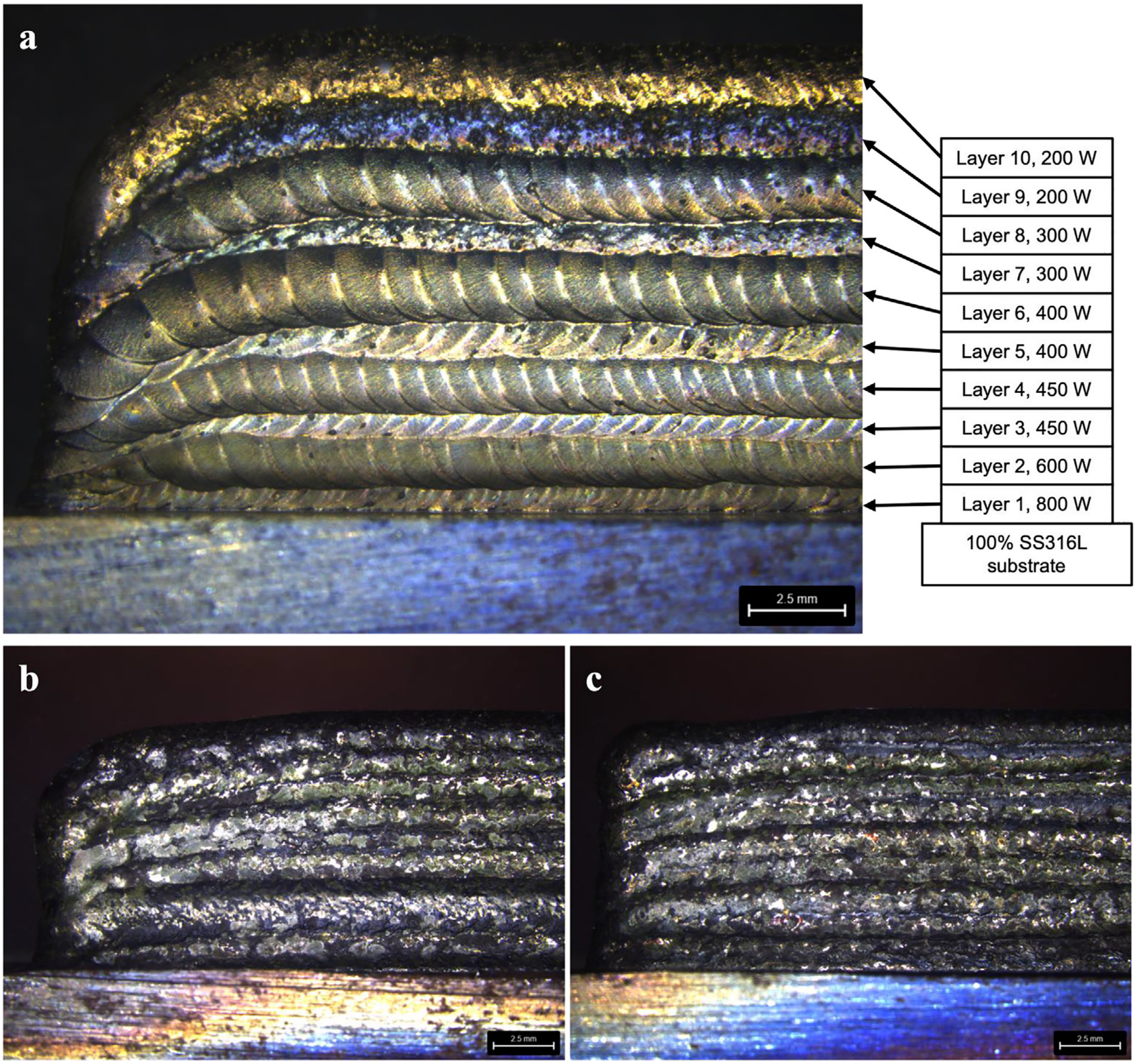

Fig. 3. Micrographs of the left area on one side of the specimen: a) 75% SS316L/25% IN 718 FGM specimen captioned by layer number and corresponding laser power used in the DED printing process; b) 100% SS316L specimen printed by DED process using the same laser power; c) 100% IN718 specimen printed by DED process using the same laser power.

pool as observed. The other suggestion for this oscillation is the different surface tension gradients between these two alloys [13,14]. However, both hypotheses would not be correct if the different kinds of powder stay well-mixed throughout the system during the entire DED process. In other words, while fabricating FGM specimens in practice, the pre-mixed powders of different types have different particle densities and particle sizes, which will lead to different particle acceleration and the separation in the powder mixture [15]. This flow behavior during the laser metal deposition will cause the uneven distribution and separation of the pre-mixed powder before and while forming the molten pool upon laser melting, which has been investigated numerically and verified experimentally [15]. For this specific study, an attempt of a fully coupled molten pool – physics simulations was made, however, that effort did not yield computational results to replicate such a phenomenon in computation; further analysis is needed to understand such a phenomenon.

4. Conclusion

This paper reports the finding of an interesting phenomenon during the DED printing process; the molten pool was found to swing with varying brightness and area while printing stainless steel 316L (75% wt.)/Inconel 718 (25% wt.) FGM. The molten pool repeated migration process was recorded by a digital camera placed above the printing head, and the ripple morphology on the surface of the printed FGM specimen caused by such molten pool swing was examined using optical micrographs. Images recorded by the camera provided a direct visualization of the molten pool in terms of the swinging path, pattern, and approximate cycling time. After analyzing the ripple morphology occurring frequency and layer thickness, it was determined that the specific material composition of stainless steel 316L and Inconel 718 caused the instability and shaking of the molten pool during the DED printing process. Potential causes for this molten pool swing are discussed based on the existing studies, including the uneven distribution and separation of the pre-mixed powder due to different particle densities. sizes, and the resulting different particle accelerations in the powder mixture. Although this phenomenon was only observed while fabricating the FGM specimen of the specific material composition in this study, such molten pool instability can occur during other laser melting deposition processes with multiple powder materials according to the proposed hypotheses. Further analysis is needed to understand such a phenomenon.

Declaration of Competing Interest

The authors declare that they have no known competing financial interests or personal relationships that could have appeared to influence the work reported in this paper.

Acknowledgments

We acknowledge the support of DoE DE-NA0003962, and NSF 1661246/1636306/1726435. Lu also acknowledges the Louis A. Beecherl Jr. Chair for additional support.

Appendix A. Supplementary data

Supplementary data to this article can be found online at https://doi.org/10.1016/j.mfglet.2022.03.002.

References

[1] Carroll BE, Otis RA, Borgonia JP, Suh J-O, Dillon RP, Shapiro AA, et al. Functionally graded material of 304L stainless steel and inconel 625 fabricated by directed energy deposition: characterization and thermodynamic modeling. Acta Mater 2016;108:46–54.

[2] Li W, Karnati S, Kriewall C, Liou F, Newkirk J, Brown Taminger KM, et al. Fabrication and characterization of a functionally graded material from Ti-6Al-4 V to SS316 by laser metal deposition. Addit Manuf 2017;14:95–104.

[3] Li W, Liou F, Newkirk J, Taminger KMB, Seufzer WJ. Investigation on Ti6Al4V-V-Cr-Fe-SS316 multi-layers metallic structure fabricated by laser 3D printing. Sci Rep 2017;7(1):7977.

[4] Li W, Zhang J, Zhang X, Liou F. Effect of optimizing particle size on directed energy deposition of Functionally Graded Material with blown Pre-Mixed Multi-Powder. Manufact Lett 2017;13:39–43.

[5] Rodriguez J, Hoefer K, Haelsig A, Mayr P. Functionally graded SS 316L to Ni-based structures produced by 3D plasma metal deposition. Metals 2019;9(6):620.

[6] Zhang J, Zhang Y, Li W, Karnati S, Liou F, Newkirk JW. Microstructure and properties of functionally graded materials Ti6Al4V/TiC fabricated by direct laser deposition. Rapid Prototyp J (just-accepted) 2018;24(4):677–87.

[7] Chen Y, Clark SJ, Huang Y, Sinclair L, Leung CLA, Marussi S, et al. In situ X-ray quantification of melt pool behaviour during directed energy deposition additive manufacturing of stainless steel. Mater Lett 2021;286:129205.

[8] Chouhan A, Aggarwal A, Kumar A. A computational study of porosity formation mechanism, flow characteristics and solidification microstructure in the L-DED process. Appl Phys A 2020;126(11):1–12.

[9] Lindenmeyer A, Webster S, Zaeh MF, Ehmann KF, Cao J. Template-bayesian approach for the evaluation of melt pool shape and dimension of a DED-process from in-situ X-ray images. CIRP Ann 2021;70(1):183–6.

[10] C.L. Coward, Electrostatic conveyor-wheel powder feeder, Google Patents, 2020.

[11] F. Anton, Method and apparatus for spinning, Google Patents, 1944.

[12] https://lasergraaf.nl/en/archive/laser-cutting-of-highly-reflective-metal-copper-silver-brass-etc/, A typical fiber laser operates at a light frequency of 1060 to 1080 nm.

[13] Anthony T, Cline H. Surface rippling induced by surface-tension gradients during laser surface melting and alloying. J Appl Phys 1977;48(9):3888–94.

[14] Niu H, Chang I. Instability of scan tracks of selective laser sintering of high speed steel powder. Scr Mater 1999;41(11):1229–34.

[15] Li W, Karnati S, Zhang Y, Liou F. Investigating and eliminating powder separation in pre-mixed powder supply for laser metal deposition process. J Mater Process Technol 2018;254:294–301.